ISSN 0511-5728
The West Indian Journal of Engineering
Vol.45, No.2, January 2023, pp.50-56

Fluid Flow and Heat Transfer Characteristics of Clerestory-Shaped Attics Heated from Below

Ola Kamiyo [a,Ψ], and Adekojo Waheed [b]

[a] Department of Mechanical Engineering, University of Lagos, Lagos, Nigeria; Email: okamiyo@unilag.edu.ng

[b] Department of Mechanical Engineering, Federal University of Agriculture, Abeokuta, Nigeria; Email: akindoye@gmail.com

[Ψ] *Corresponding Author*

(Received 28 June 2022; Revised 13 October 2022; Accepted 22 November 2022)

Abstract: *In this study, a finite volume analysis of the aerodynamics and heat transfer in attics of a clerestory roof design with pitch angles 14º, 18º, 30º and 45º and Rayleigh number range $3 \times 10^5 \leq Ra \leq 2 \times 10^7$ is carried out. The shape of the enclosure has strong influence on the structure of the flow and temperature fields. The flow field is characterised by counter-rotating vortices enclosed by aerodynamic boundary layers. The size, strength and direction of rotation of the cells are controlled by the forces propelling the thermal plumes and the cold jets. The reduction of the number and size of the counter-rotating cells and their formation within the enclosures provide an analogous reduction of the total heat transfer rate as the roof pitch angle increases. The velocity and temperature profiles across midheight and midlength of the enclosures enable the prediction of appropriate position in the attic with the right condition to place sensitive items. On the heat transfer, the relationship between the mean Nusselt number and the Rayleigh number is presented in form of a correlation. Results obtained in the study are of significance to building engineers engaged in the analysis and design of building attics and tropical agriculturalists for the control of produce drying rates.*

Keywords: *Heat transfer, heated below, natural convection, pitch roof, clerestory-shaped*

Nomenclature

AR	Aspect ratio, AR =2H/L
g	Acceleration due to gravity, m/s²
H	Height of enclosure, m
k	Thermal conductivity, W/mK
L	Length of enclosure, m
Pr	Prandtl number
Ra	Rayleigh number
T	Temperature, K
T_C	Temperature at the cold wall, K
T_H	Temperature at the hotwall, K
u	Velocity in x-axis, m/s
U, V	Dimensionless velocity
V	Velocity in y-axis, m/s
X, Y	Dimensionless Cartesian coordinates

Greek symbols

α	Thermal diffusivity, m²/s
β	coefficient of thermal expansion, K
θ	Dimensionless temperature
ν	Kinematic viscosity, m²/s
ρ	Density, kg/m³
ϕ	Pitch angle, degrees

1. Introduction

The study of transport process in the attics has gained enormous attention over the years due to its vast areas of its applications. For example, in the rural communities of Sub-Saharan Africa, agricultural produce is often carefully arranged within the attic either for drying or for long-term storage for future use. In many Europeans cities, the attic space is sometimes used as a penthouse or for storage of items not being frequently used. The thermal characteristics of the attics vary with the climatic region and the nature of the heat flow in and out of an attic space generally affects the environmental condition of the space directly below it. As a result, the knowledge of the heat convection within the attic is necessary in order to correctly predict its effect on the thermal comfort and energy efficiency of the system.

The geometry of an attic depends on the shapes and orientation of the pitch roofs which differ from one part of the world to the other. Foundational experimental and numerical works on regular triangular-shaped pitch roofs include those of Flack (1980), Akinsete and Coleman (1982) and Poulikakos and Bejan (1983). Using the Galerkin weighted residual finite element method, Del Campo *et al*. (1988) obtained steady-state solutions for all possible seven thermal boundary conditions for a triangular enclosure. They observed that the intensity and rate of heat transfer in the enclosures heated from the base wall are much higher than in the enclosures heated from the side walls. The extensive reviews carried out by Kamiyo *et al*. (2010) and Saha and Khan (2011) indicate

https://doi.org/10.47412/XIID6834

that most studies carried out up till that time on heat transfer in roofs were of isosceles triangular shapes despite the existence of many buildings with complex-shaped roofs.

Thereafter, a number of authors have studied unconventional attics. Yesiloz and Aydin (2013) performed experimental and numerical analyses of natural convection in a right-angled triangular-shaped enclosure isothermally heated at the base, cooled on the vertical wall while the inclined wall is adiabatic. The flow structure shows that the vortex at the middle of the enclosure widens while the shape also deteriorates. As the Rayleigh number (*Ra*) increases, thermal stratification becomes more intensive near the heat transfer surfaces. Using the Bejan's heatline approach, Basak *et al*. (2013) investigated natural convection in similar right-angled triangular enclosures but with a concave and convex inclined wall. The results show that for all parameters considered, thermal mixing in the enclosure with the convex hypotenuse is higher than in the concave case. Mirabedin (2016) developed a correlation for Nusselt number in terms of aspect ratio and Rayleigh number for heat transfer in the same right-angled triangular enclosure. Sieres *et al.* (2016) applied analytical and numerical methods to study laminar natural convection of air in vertical upright–angled triangular enclosures to show that, at low *Ra* and for lower angles, the heat transfer rate increases but at high *Ra,* it remains constant. Das *et al.* (2017) reviewed natural enclosure in some other irregular shapes.

Other complex roofs that have been investigated include inclined triangular (Mahmoudi *et al.*, 2013), dome (Das and Morsi, 2002), gable (Amrani *et al.*, 2017), trapezoidal (Mehryan *et al.*, 2020), section-triangular prismatic (Cui *et al*., 2019), vaulted (Elnokaly *et al.*, 2019), paraboloid roof (Colliers *et al.*, 2020) and flat-top (Kamiyo, 2021). In spite, there are other common complex roofs that have not been adequately studied. The clerestory-shaped roof is one of such. This study, therefore, aims to investigate the aerodynamics and heat transfer within the attic of a clerestory-shaped roof under winter condition.

2. Methods

A long horizontal air-filled attic with a clerestory-shaped triangular cross-section shown in Figure 1 is investigated in this work. The cross-section is simply an isosceles triangle truncated by a vertical line. In real life, the location and height of the vertical wall vary. In this study, the vertical wall is at two-third of the base length and its height, h, is half of the enclosure height, H. Based on Penot and N'Dame (1992), since the width of the roof is less than half of its length, the flow and thermal fields could be taken as two-dimensional.

The air within the enclosure is regarded as a viscous, incompressible and Newtonian fluid. The properties of the fluid are assumed constant except change of density with temperature during buoyancy. Hence, the Boussinesq approximation is employed (Ridouane *et al*., 2005).

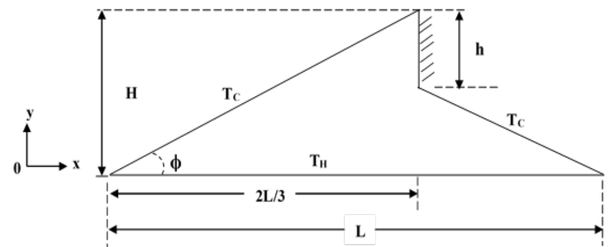

Figure 1. Physical Model

There is no internal heat generation in the cavity and all its walls are impermeable. The flow and thermal fields are taken to be steady. Since the size of a real life roof and thermal conditions of the environment vary, the computational domain dimensions and boundary conditions are normalised. The equations governing the steady, laminar natural convective flow and heat transfer are expressed in dimensionless form, with Boussinesq approximation, as:

Continuity:

$$\frac{\partial U}{\partial X}+\frac{\partial V}{\partial Y}=0 \tag{1}$$

X-Momentum:

$$U\frac{\partial U}{\partial X}+V\frac{\partial U}{\partial Y}=-\frac{\partial P}{\partial X}+\mathrm{Pr}\left(\frac{\partial^2 U}{\partial X^2}+\frac{\partial^2 U}{\partial Y^2}\right) \tag{2}$$

Y-Momentum:

$$U\frac{\partial V}{\partial X}+V\frac{\partial V}{\partial Y}=-\frac{\partial P}{\partial Y}+\mathrm{Pr}\left(\frac{\partial^2 V}{\partial X^2}+\frac{\partial^2 V}{\partial Y^2}\right)+RaPr\theta \tag{3}$$

Energy:

$$U\frac{\partial \theta}{\partial X}+V\frac{\partial \theta}{\partial Y}=\left(\frac{\partial^2 \theta}{\partial X^2}+\frac{\partial^2 \theta}{\partial Y^2}\right) \tag{4}$$

where

$$X=\frac{x}{L},\ Y=\frac{y}{L},\ V=\frac{vL}{\alpha},\ U=\frac{uL}{\alpha},\ \theta=\frac{T-T_C}{T_H-T_C},$$

$$P=\frac{pL^2}{\rho\alpha^2},\ Pr=\frac{\nu}{\alpha},\ \text{and}\ \ Ra=\frac{g\beta(T_H-T_C)H^3}{\alpha\nu}.$$

The boundary conditions are:

Velocity:

$U = V = 0$ *(no slip condition along the walls)*

Temperature:

$\theta = 1$ *(isothermal hot ceiling)*

$\theta = 0$ (isothermal cold inclined walls)

$d\theta/dx = 0$ *(adiabatic vertical wall)*

Roof pitch angles of 14°, 20°, 25°, and 35° that are common and within the standard roof pitch range were studied. The parametric details are as stated in Table 1.

Table 1: Parametric Details of the Enclosures

Pitch Angle (ϕ)	14°	18°	30°	45ᵖ
Aspect Ratio (*AR*)	0.25	0.325	0.58	1.00
Rayleigh Number (*Ra*)	3 x10^5	7 x10^5	4 x 10^6	2 x 10^7

Figure 2. Computational Grid for the 30º - Pitch Enclosure

Fine unstructured triangular meshes, shown in Figure 2 for the 30º pitch enclosure, were used for the computational domains. The finite-volume based ANSYS FLUENT© CFD package was used to solve numerically the coupled nonlinear partial differential equations (1) - (4) governing the natural convective heat transfer problem. The pressure-velocity coupling in the equations was resolved by the SIMPLE algorithm. The QUICK scheme in the software was employed to spatially discretise the momentum and energy equations. PRESTO scheme was used for the pressure interpolation. The conservation equations were solved iteratively till convergence was achieved. The convergence criterion for the continuity equation was set at 10^{-5} while that for the momentum and energy equations was set at 10^{-7}. To ensure the accuracy of the solution scheme and to determine an appropriate grid density, a grid independence test was carried out using the value of the average Nusselt number of the hot base wall relative to the number of elements. The outcome of some of the numerical runs is as shown in Table 2 for the 14^0-pitch enclosure.

Table 2. Grid Independence Test for the 14° - Pitch Enclosure

Number of elements	45,255	50,373	55,895	61,215
$\overline{Nu}$	16.45	19.75	22.32	22.46

Ability of the commercial CFD package used to effectively carry out the computation of the present study is premised on the work of Yesiloz and Aydin (2013). They compared the results of the numerical analysis of laminar natural convection in a right-angled triangular enclosure heated from below carried out using ANSYS FLUENT with the results of an experiment with the same configuration and Rayleigh number range of 10^3 to 10^7. The results are found to be in good agreement.

3. Results and Discussion

The steady state results obtained for the fluid flow and heat transfer within the enclosures are presented in Figures 3-8. These include the streamlines, contour plots of the velocity and temperature, and the graphical plots of the variations of the velocity and temperature across some sections. Others are the graphical plot of the mean Nusselt number variation along the hot base wall. The reference velocity is $U = \sqrt{g\beta(T_H - T_C)H}$ and the dimensionless temperature, $= {(T - T_C)}/{(T_H - T_C)}$; hence both range from zero to one. The length, L of the base wall and the enclosure height H scale the x-coordinate and y-coordinate, respectively.

3.1 Thermal and Flow Fields

The thermophysical structure of the system is depicted by hot, less-dense air that rises in form of a plume from the heated base wall through the attic and hits an upper inclined cold wall. In reaction to the buoyant force, the upward flow bifurcates in either direction along the inclined wall. After losing part of its heat content, the fluid becomes denser. Consequently, the flow, under gravity, detaches from the inclined wall, goes down to the base wall to regain heat and repeat the process. The size, strength and direction of rotation of the cells are determined by the plume's location and the buoyant force propelling it. The vertical wall distorts the flow field around it and, in some cases, caused flow detachment. Also, the lengths and the difference in the subtending angles of the cold inclined walls affect the rate of heat exchange with the hot horizontal base wall thereby making the cell arrangement asymmetric. The temperature fields are strongly influenced by the airflow patterns in the enclosures.

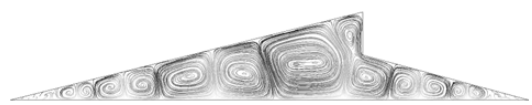

(a) 14º

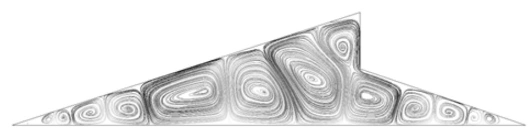

(b) 18º

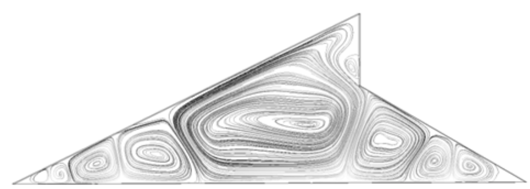

(c) 30º

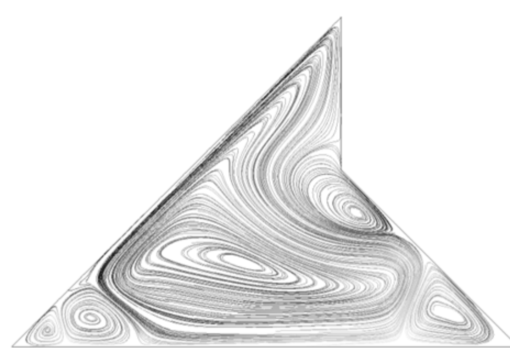

(d) 45º

Figure 3. Streamlines for Different Pitch Angles

In Figure 3a for the 14^0-pitch enclosure, the flowfield shows ten counter-rotating cells that are asymmetrically arranged; six on the left and four on the right. The size and strength of the cells reduce from the midsection to the bottom corners. Upon hitting the vertical wall, the plume rises directly below it splits. A flow detachment occurs. As a result, a secondary, weak-strength, clockwise-rotating cell is formed at the upper corner. At the bottom corners, the nearness of the hot and cold walls makes conduction to dominate; the area becomes smaller with increasing roof pitch angle. In the 18^0-pitch enclosure, Figure 3b, due to a marginally increased space area, the airflow structure remains practically unchanged but the cells have become bigger.

In the 30^0 pitch enclosure, Figure 3c, some of the cells have merged, leaving only seven. Three cells at the midsection merged with the one at the upper vertex to form a big vortex that is distorted by the vertical wall. The central cell rotating anti-clockwise became the main force in the flow as it drags down cold air along almost half of the left inclined wall. In Figure 3d, with more space to roam in the 45°-pitch enclosure, the large central vortex appears to have 'swallowed up' more cells. Others cells have also grown larger and have gained higher convective strengths. In each of the enclosures, the rotating speed of a cell reduces with the cell size. The multi-cellular flow pattern obtained in this study concurs with the results of Cui *et al*. (2015 and 2019). It is also similar to that reported in the experiments conducted in an isosceles triangular enclosure heated from the base wall by Holtzman *et al.* (2000).

Figure 4 shows the contour plots of the air velocity for each of the enclosures. In each cell, there are two main regions: the outer and core regions. In the outer region which falls around the periphery of a cell's circumference, the values of velocity are relatively high. On the other hand, the core region is somehow quiescent. The velocity values are also high along the plumes, in between adjacent cells and along the walls.

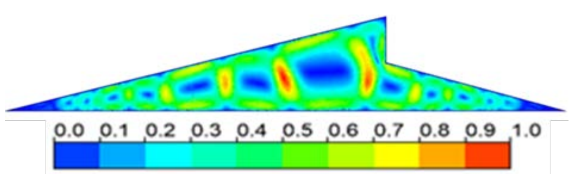

(a) 14º

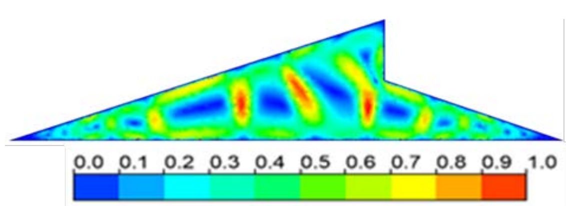

(b) 18º

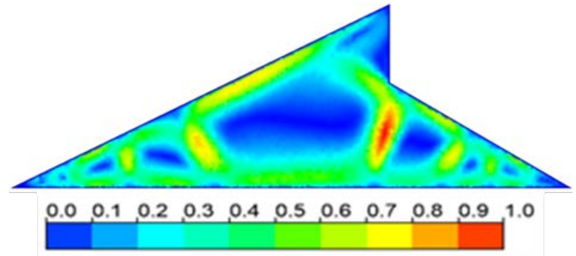

(c) 30º

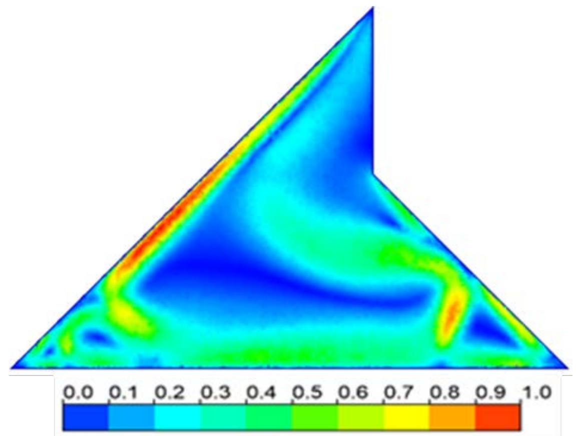

(d) 45º

Figure 4. Velocity Contour Plots for Different Pitch Angles

In Figure 5, the variation of the values of air velocity along the vertical cross-section at X = 0.5L is presented for the roof pitch enclosures. The profiles show air velocity at the part of the cells that falls on the wall. The vertical line at X = 0.5L passes through the largest cell in all the enclosures. The velocity is relatively high at the edge of the cell and low at the core. The higher the roof pitch, the higher the velocity of rotation.

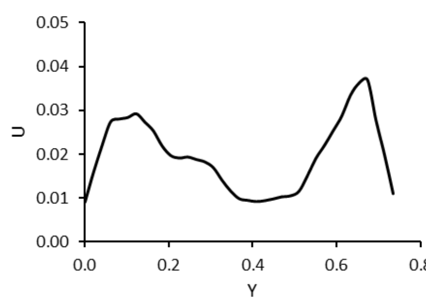

(a) 14º

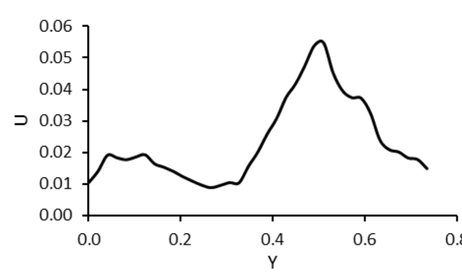

(b) 18º

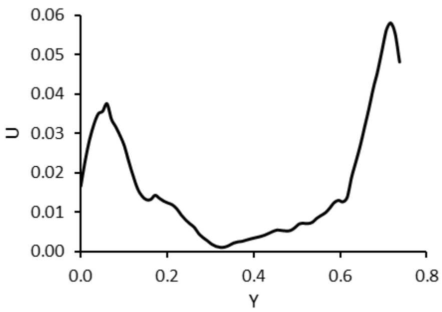

(c) 30 º

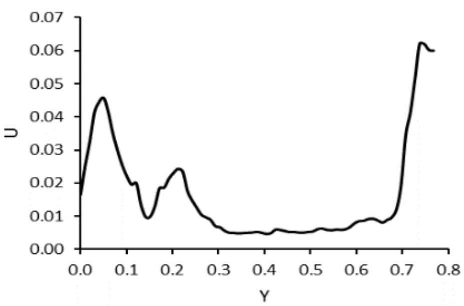

(d) 45 º

Figure 5. Air Velocity along Vertical *X*=0.5L Cross-section of Each Enclosure

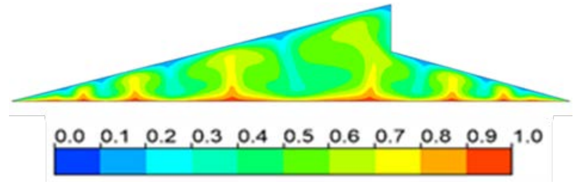

(a) 14º

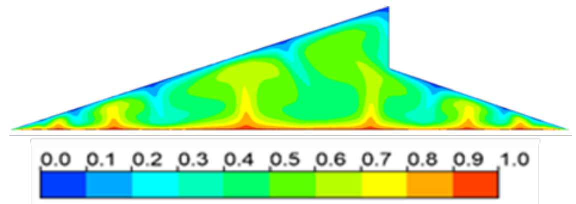

(b) 18º

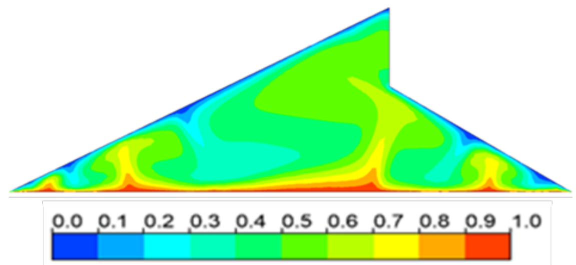

(c) 30º

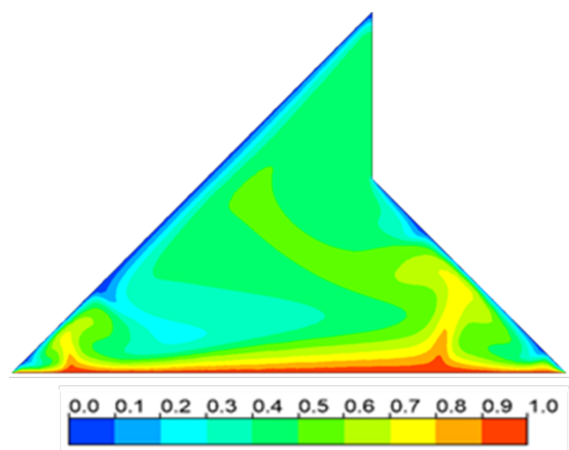

(d) 45º

Figure 6. Temperature Contour Plots for Different Pitch Angles

Figure 6 shows the contour plots of the temperature distribution within the enclosures. The thermal field is characterised by rising hot plumes from the heated base wall and of cold jets descending from the cold upper walls. The system results in a mixture of hot and cold air within the attics. A plume and a jet fall between two counter-rotating cells. Due to the peculiar shape of the enclosure, the thermal field is strongly influenced by the strength of the convection currents and the distortion of the airflow by the vertical wall. The development of plumes in this study is in consonant with the report of Cui et al., (2015). In the 14^0 roof pitch enclosure, Figure 6a, the high number of counter-rotating cells leads to thorough mixing of air. As the pitch angle increases however, the volume of cold air that is being heated by the same base wall length becomes larger. Hence, the heating effect and thus the average temperature across the enclosure reduce. In all but the 45^0 pitch enclosure, the vertical wall falls on the path of a plume of hot air, hence, being constantly heated. Therefore, whether used as a penthouse window or a skylight, the warm vertical wall reduces snow thickness on it.

The temperature profiles along the vertical cross-section at *X*= 0.5L are presented in Figure 7 for each enclosure. The variation of the temperature values follows the part of a cell that falls along the lines. The plots clearly show the thermal boundary layers along the base wall (at *Y* = 0) and the opposing inclined wall. For each of the vertical cross-section, the thickness of the boundary layer reduces as the roof pitch increases.

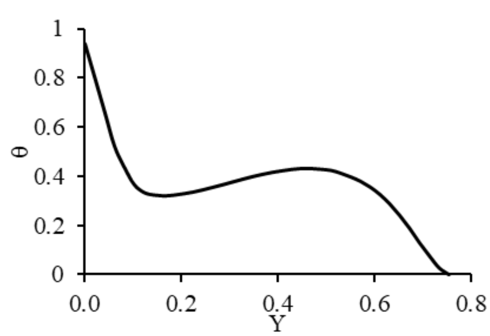

(a) 14 º

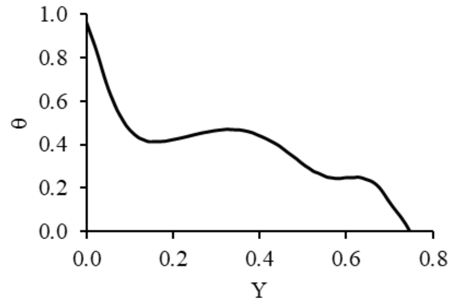

(b) 18 °

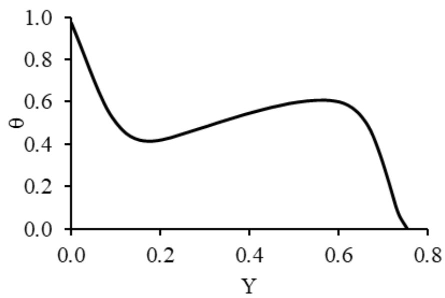

(c) 30 °

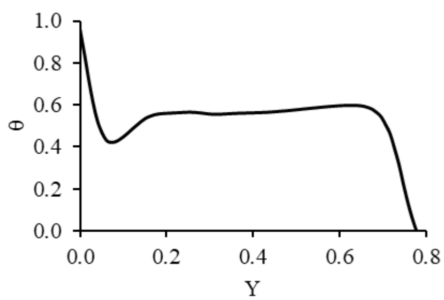

(d) 45 °

Figure 7. Temperature along vertical *X*=0.5L cross-section of each enclosure

3.2 Heat Transfer

The rate of the flow of heat from the hot base wall into the air-filled attic can be represented by the average heat transfer rate over the hot base wall depicted by the mean Nusselt number defined as,

$$\overline{Nu} = \frac{\bar{q}\, L}{k_f\, \Delta T} \qquad (5)$$

where $\overline{q}$ is the mean value of the local surface heat flux across *L*. The plot of the mean Nusselt number ($\overline{Nu}$) of the hot basewall against the Rayleigh number (*Ra)* for the 14° roof pitch enclosure is presented in Figure 8 where $\overline{Nu}$ increases with Ra. This agrees with literature on the subject (Cui et al., 2019).

The correlation between the $\overline{Nu}$ *and Ra* for the heat exchange along the hot wall of the 14° roof pitch enclosure is as indicated in Equation (6).

$$\overline{Nu} = 28.1\mathrm{Ra}^{0.232} \qquad (6)$$

The relation agrees closely with literature which suggests $\overline{Nu} \sim Ra^{1/4}$ for laminar flow cases. For the clerestory enclosure with roof pitch of 45^0 and *Ra* value of 2 x 10^7 in this study, the $\overline{Nu}$ value for the hot base wall is 34. At the same pitch angle and Ra of 10^7, Cui et al. (2019) got 32 for $\overline{Nu}$ for the hot base wall of a standard triangle.

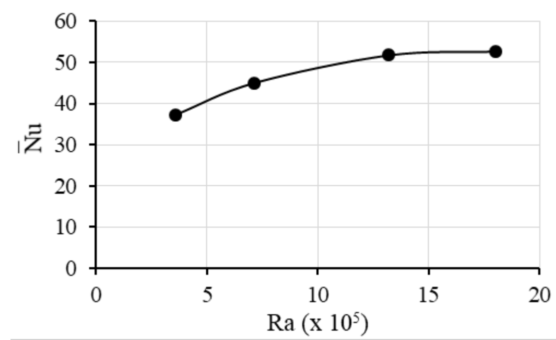

Figure 8: Mean Nusselt Number of the Base Wall against Rayleigh Number for 14^0-Pitch.

For the same *Ra* range, 5 x 10^7, Anderson *et al* (2010) obtained $\overline{Nu}$ value of 35 for the hot inclined wall of an isosceles triangular cavity. The implication of the results of this investigation is that, in temperate climate, heat loss across the ceiling into the roof can be minimised when the angle of the roof pitch is rather high. If roof of low-pitch is to be used, the ceiling insulation should be thick and of high quality.

4. Conclusion

A finite volume analysis of fluid flow and heat transfer in clerestory-shaped attics heated from below has been investigated. The shape of the enclosure has strong influence on the flow and temperature fields. As common to enclosures heated from the base wall, the flow field is characterised by counter-rotating vortices enclosed by aerodynamic boundary layers. The asymmetrically-arranged cells increase in number with the roof pitch angle. The size, strength and direction of rotation of the cells are controlled by the buoyant force propelling the thermal plumes from the bottom wall and the gravitational force on the cold jets from the top inclined walls. The reduction of the number and size of the counter-rotating cells and their formation within the enclosures provide an analogous reduction of the total heat transfer rate for increasing roof pitch. The temperature field is influenced by the flow pattern.

At low roof pitch angles, multi-cellular flow structure controls the transport processes within the enclosures leading to thorough mixing of air and hence, more uniform attic temperature. The values of velocity and temperature plotted across midheight and midlength of the enclosures displayed sinusoidal order. These profiles enable the prediction of suitable position for the placement of sensitive items on the rooftop. On the heat transfer, the correlation relating the mean Nusselt number and the Rayleigh number agrees with literature.

References:

Akinsete, V.A. and Coleman, T.A., (1982), "Heat transfer by steady laminar free convection in triangular enclosures", *International Journal of Heat Mass Transfer*, Vol. 25, pp. 991.

Amrani, A., Dihmani, N., Amraqui, S. and Mezrhab, A., (2017) "Analysis of combined natural convection and thermal radiation heat transfer in a triangular shaped roof for hot climates", *Journal of Materials and Environmental Sciences*, Vol.8, No.8, pp. 3013-3027.

Anderson, T.N., Duke, M. and Carson, J.K., (2010), "Experimental determination of natural convection heat transfer coefficients in an attic shaped enclosure", *International Communications in Heat and Mass Transfer*, Vol.37, No.4, pp.360-363.

Basak, T., Anandalakshmi, R. and Biswal, P. (2013), "Analysis of convective heat flow visualisation within porous right angled triangular enclosures with a concave/convex hypotenuse", *Numerical Heat Transfer, Part A: Applications*, Vol.64, No. 8, pp. 621-647.

Colliers, J., Degroote, J., Mollaert, M., and De Laet, L. (2020), "Mean pressure coefficient distributions over hyperbolic paraboloid roof and canopy structures with different shape parameters in a uniform flow with very small turbulence", *Engineering Structures*, Vol.205, 110043.

Cui, H., Xu, F., Saha, S.C. and Liu, Q. (2019), "Transient free convection heat transfer in a section-triangular prismatic enclosure with different aspect ratios", *International Journal of Thermal Sciences*, Vol.139, pp.282-291.

Cui, H., Xu, F., and Saha, S.C. (2015), "A three-dimensional simulation of transient natural convection in a triangular cavity", *International Journal of Heat and Mass Transfer*, Vol. 85, pp.1012-1022.

Das, D., Roy, M., and Basak, T. (2017), "Studies on natural convection within enclosures of various (non- square) shapes - A review", *International Journal of Heat and Mass Transfer*, Vol.106, pp.356-406.

Das, S., and Morsi, Y., (2002), "Natural convection inside dome shaped enclosures", *International Journal of Numerical Methods for Heat and Fluid Flow*, Vol.12, No.2, pp.126-141.

Del Campo, E.M., Sen, M., and Ramos, E. (1988), "Analysis of laminar natural convection in triangular enclosures", *Numerical Heat Transfer*, Vol. 13, pp.353-372.

Elnokaly, A., Ayoub, M., and Elseragy, A. (2019), "Parametric investigation of traditional vaulted roofs in hot-arid climates", *Renewable Energy*, Vol.138, pp.250-262.

Flack, R.D., (1980), "The experimental measurement of natural convection heat transfer in triangular enclosures heated or cooled from below", *Journal of Heat Transfer*, Vol.102, pp.770-772.

Haese, P.M., and Teubner, M. D., (2002), "Heat exchange in an attic space", *International Journal of Heat and Mass Transfer*, Vol. 45, pp.4925-4936.

Holtzman, G.A., Hill, R.W., and Ball, K.S., (2000), "Laminar natural convection in isosceles triangular enclosures heated from below and symmetrically cooled from above", *Journal of Heat Transfer*, Vol. 122, No.3, pp. 485-491.

Kamiyo, O.M., Angeli, D., Barozzi, G.S., Collins, M.W., Olunloyo, V.O.S., and Talabi, S.O. (2010), "A comprehensive review of natural convection in triangular enclosures", *Journal of Applied Mechanics Review*, Vol.63, No.6, 060801, 13 pages.

Kamiyo, O. (2021), "Airflow and heat transfer analysis within flat-top roofs heated from below", *West Indian Journal of Engineering*, Vol.43, No.2, pp.4-11.

Mahmoudi, A., Mejri, I., Abbassi, M.A., and Omri, A., (2013), "Numerical study of natural convection in an inclined triangular cavity for different thermal boundary conditions: application of the lattice Boltzmann method", *Fluid Dynamic Material Process*, Vol. 9, pp.353-388.

Mehryan, S.M., Mohammad, G., Reza, K.F., Ahmad, H., and Mohsen, I., (2020), "Free convection in a trapezoidal enclosure divided by a flexible partition", *International Journal of Heat and Mass Transfer*, 149:119186, 14 pages.

Mirabedin, S. (2016), "CFD modelling of natural convection in right–angled triangular enclosures", *International Journal of Heat Technology*. Vol. 34, No.3, pp.503-506.

Penot, F., and N'Dame, A., (1992), "Successive bifurcations of natural convection in a vertical enclosure heated from the side", *Proceedings of 3rd UK National Conference and First European Conference on Thermal Sciences*, Birmingham, UK, Vol. I, pp.507-513.

Poulikakos, D., and Bejan, A., (1983), "The fluid dynamics of an attic space", *Journal of Fluid Mechanics*, Vol. 131, pp.251-269.

Ridouane, E. H., Campo, A., and McGarry, M., (2005), "Numerical computation of buoyant airflows confined to attic spaces under opposing hot and cold wall conditions", *International Journal of Thermal Sciences*, Vol.44, pp.944-952.

Saha, S.C. (2011), "Unsteady free convection in a triangular enclosure under isothermal heating", *Energy and Building*, Vol. 43, pp.701-709.

Saha, S.C. and Khan, M.M.K., (2011), "A review of natural convection and heat transfer in attic-shaped space", *Energy and Building*, Vol. 43, pp.2564-2571.

Sieres, J., Campo A., Martinez-Suarez, J.A., (2016), "Natural convection air flow in vertical upright-angled triangular cavities under realistic thermal boundary conditions", *Journal of Thermal Science*, Vol. 20, No.5, pp.1407-1420.

Yesiloz, G. and Aydin, O., (2013), "Laminar natural convection in right-angled triangular enclosures heated and cooled on adjacent walls", *International Journal of Heat and Mass Transfer*, Vol.60, pp.365-374.

Authors' Biographical Notes:

Ola Kamiyo *is a Senior Lecturer at the Department of Mechanical Engineering, University of Lagos, Lagos, Nigeria where he is actively involved in both teaching and research. Dr. Kamiyo holds a BSc, MSc and PhD degrees in Mechanical Engineering at the Department of Mechanical Engineering, University of Lagos. He was a visiting Research Fellow at the Department of Engineering "Enzo Ferrari", University of Modena and Reggio Emilia, Modena, Italy. His areas of research interest include heat transfer in enclosures and thermal properties of novel building materials.*

Adekojo Waheed *is a Professor of Thermofluids and Fluid Mechanics at the Department of Mechanical Engineering, Federal University of Agriculture Abeokuta, Nigeria where he is actively involved in both teaching and research. Professor Waheed holds a Doctor of Engineering Science Degree (Dr. Eng. Sc.) in Mechanical Engineering, from Aachen University of Technology (RWTH) Aachen; Germany. Master in Engineering (M. Eng.) in Mechanical Engineering from the University of Ilorin, Nigeria and Bachelor of Engineering, (B. Eng.) in Mechanical Engineering from the University of Ilorin, Nigeria. He was a Commonwealth Fellow at the Department of Mechanical Engineering, University of Bath, Claverton Down, Bath, United Kingdom. His areas of research interest include heat transfer and fluid mechanics.*

■